Atmospheric chemistry of FO2 radicals. Reaction with Ch4, O3, No, No2, and Co at 295 K

ARTICLE *in* THE JOURNAL OF PHYSICAL CHEMISTRY · JULY 1994

Impact Factor: 2.78 · DOI: 10.1021/j100078a014

Atmospheric Chemistry of FO_2 Radicals: Reaction with CH_4, O_3, NO, NO_2, and CO at 295 K

Jens Sehested, Knud Sehested, and Ole John Nielsen*

Chemical Reactivity Section, Environmental Science and Technology Department, Risø National Laboratory, DK-4000 Roskilde, Denmark

Timothy John Wallington*

Sci. Res. Labs. E3083, Ford Motor Co. P.O. 2053, Dearborn, Michigan 48121

*Received: February 10, 1994; In Final Form: May 12, 1994**

Using pulse radiolysis combined with UV absorption spectroscopy, upper limits for the rate constants of the reaction of the FO_2 radical with O_3, CH_4, and CO were determined to be $<3.4 \times 10^{-16}$, $<4.1 \times 10^{-15}$, and $<5.1 \times 10^{-16}$ cm^3 molecule^{-1} s^{-1}, respectively. The rate constants for the reactions of FO_2 radicals with NO and NO_2 were measured: $FO_2 + NO \rightarrow FNO + O_2$ (10a); $FO_2 + NO_2 \rightarrow$ products (11). The rate constants for reactions 10 and 11 were determined to be $(1.47 \pm 0.08) \times 10^{-12}$ and $(1.05 \pm 0.15) \times 10^{-13}$ cm^3 molecule^{-1} s^{-1}, respectively. Reaction 10a was found to give FNO in a yield of 100 ± 14%. As a part of this work, an upper limit of the reaction of FO radicals with O_3 was determined to be $<1.2 \times 10^{-12}$ cm^3 molecule^{-1} s^{-1}. Results are discussed in the context of the atmospheric chemistry of the FO_2 radical and hydrofluorocarbons.

Introduction

Recognition of the adverse environmental effect of chlorofluorocarbon (CFC) release into the atmosphere has led to an international agreement to phase out CFCs by the end of 1995. Efforts have been made to find environmentally acceptable alternatives. Among these alternatives are hydrofluorocarbons (HFCs). Prior to their large-scale industrial use, the environmental impact of HFCs must be investigated.

HFCs, when released into the atmosphere, will react with OH to form alkyl radicals which will, in turn, react with O_2 to form peroxy radicals.[1,2] The degradation of these fluorinated peroxy radicals in the atmosphere is known to produce a variety of products and radicals such as FO_2, FO, CF_3O, CF_3O_2, CF_2HO_2, CFH_2O_2, CF_3OH, FNO, CF_3COF, CF_3COH, HCOF, CF_2O, and HF.[1,2]

It has been discussed whether the CF_3O and CF_3O_2 radicals could destroy ozone in a catalytic cycle.[3] It is now well accepted that the ozone depletion effect of CF_3O_x radicals is negligible.[3,4] Attention has also been drawn to the atmospheric chemistry of the FO_x radicals. It has been suggested by Francisco and Su[5] and Francisco[6] that FO_2 and FO radicals formed in the atmospheric degradation of HFCs could destroy ozone in chain reaction processes:

$$FO + O_3 \rightarrow FO_2 + O_2 \quad (1)$$

$$FO_2 + O \rightarrow FO + O_2 \quad (2)$$

$$\text{net: } O + O_3 \rightarrow 2O_2$$

and

$$FO + O_3 \rightarrow FO_2 + O_2 \quad (1)$$

$$FO_2 + O_3 \rightarrow FO + 2O_2 \quad (3)$$

$$\text{net: } O_3 + O_3 \rightarrow 3O_2$$

A necessary but not sufficient condition for these two ozone destruction cycles to be efficient is that the FO_2 radical reacts rapidly with O_3 or O and that the loss processes for FO_x radicals are slow. Some reactions of the FO_2 radical are investigated in this work.

The equilibrium between F atoms, O_2, and FO_2 has been studied by Pagsberg et al.,[7] Lyman and Holland,[8] Ellermann et al.,[9] and Hippler.[10]

$$F + O_2 + M \rightleftharpoons FO_2 + M \quad (4,-4)$$

The following values have been reported: Pagsberg et al.,[7] $k_4 = 4.4 \times 10^{-33}$ cm^6 molecule^{-2} s^{-1} (298 K) and $K_p = 3.2 \times 10^{-25} \exp(6100/T)$ cm^3 molecule^{-1}; Lyman and Holland,[8] $k_4 = (3.1 \pm 0.3) \times 10^{-33}$ cm^6 molecule^{-2} s^{-1} and $K_p = 1.2 \times 10^{-15}$ (298 K) cm^3 molecule^{-1}; Ellermann et al.,[9] $k_4 = (1.9 \pm 0.3) \times 10^{-13}$ cm^3 molecule^{-1} s^{-1} (295 K, 1 bar SF_6); Hippler et al.,[10] $K_p = 1.17 \times 10^{-25} \exp(6712/T)$ cm^3 molecule^{-1}. In the following, the value of k_4 from Pagsberg et al.[7] and the K_p from Hippler[10] will be used.

The objective of this work is to study atmospherically significant reactions of the FO_2 radical. We have studied reactions of the FO_2 radical with NO, NO_2, CO, CH_4, and O_3 using pulse radiolysis coupled with time-resolved UV absorption spectroscopy.

Experimental Section

Two setups using pulse radiolysis coupled with time-resolved UV absorption spectroscopy were used in the present work. In the first setup a Febetron 705B accelerator was used to initiate the reactions. This experimental system has been described in detail previously[11,12] and has been used routinely for several years. The second setup applied a linear 10 MeV electron accelerator to initiate the reactions in a new 0.33 L stainless steel high-pressure cell. Results from this setup have not been reported previously in the literature. Both experimental setups are described below.

In the first system, radicals were produced in a 1 L stainless steel reaction cell using a 30 ns pulse of 2 MeV electrons from a Febetron 705B field emission accelerator. Pressures of up to 1 bar could be used in the reaction cell. The pressure was measured by a Baratron absolute membrane manometer. A chromel/alumel thermocouple measured the temperature inside the reaction cell close to the center.

The gas mixture was analyzed using UV light from a pulsed xenon lamp. The light beam from the xenon lamp was reflected 3, 7, or 11 times in the gas cell by internal White-type optics,

* Abstract published in *Advance ACS Abstracts*, June 15, 1994.

0022-3654/94/2098-6731$04.50/0

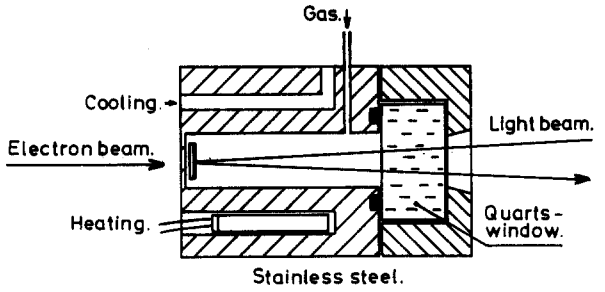

Figure 1. Outline of the high-pressure cell.

giving total optical pathlengths of 40, 80, or 120 cm. The analyzing light was passed into a McPherson 1 m grating monochromator operated at a spectral resolution of 0.8 nm and was detected by a Hamamatsu photomultiplier coupled to a Biomation digitizer. Data handling and storage were performed using a PDP11 computer.

In Figure 1 an outline of the high-pressure cell is shown. The cell is a stainless steel gas cell built for pressures up to 150 bar. Partial pressures of less than 1 bar were measured by a Juno 4ADM-22 pressure transducer coupled to a Juno PDA-48/k instrument. Pressures above 1 bar were measured by a Juno 4AP-30 pressure transducer coupled to a 4PDE-48 instrument. The cell may be heated up to 590 K, but in the present experiments, ambient temperature, 295 K, was used. Reactions were initiated by a 10 MeV HRC Linarc electron accelerator delivering a 0.5–4 μs electron pulse into the reaction cell. To obtain acceptable S/N ratios, up to five electron pulses were added. No changes in the observed transients were detected by comparing the obtained transients from the first and the last electron pulses.

The electron beam enters the cell through a thin metal window of 1.5 mm stainless steel at the left side of the cell. The diameter of the electron beam was close to the diameter of the cell, ensuring that the radiation was evenly distributed on the area entering the cell. The longitudinal distribution of radiation in the cell is also uniform since only a small fraction of the radiation is absorbed in the cell.

A 150 W Varian xenon lamp delivered the analyzing light. The xenon lamp could be pulsed to obtain better signal to noise ratios if a full time scale of less than or equal to 2 ms was applied. The analyzing light entered the cell through a quartz window and was reflected by a mirror mounted in the cell, giving a total optical pathlength of 20 cm. The light was detected by a Perkin-Elmer double-quartz prism monochromator with an optical resolution of 2–5 nm, and a IP28 photomultiplier and a LeCroy 9400 digital oscilloscope. Data handling and storage were performed using a IBM personal computer.

The gas mixtures used for both setups contained SF_6 in great excess. F atoms are known to be produced upon radiolysis of SF_6 with high-energy electrons:[12]

$$SF_6 + 2 \text{ or } 10 \text{ MeV } e^- \rightarrow F + \text{products} \quad (5)$$

The yield of F atoms has been determined routinely[13,14] in the first system by radiolysis of gas mixtures of CH_4, O_2, and SF_6 and subsequent observation of the absorbance at 260 nm ascribed to CH_3O_2 formed by reaction 5 and the following two reactions:

$$F + CH_4 \rightarrow CH_3 + HF \quad (6)$$

$$CH_3 + O_2 + M \rightarrow CH_3O_2 + M \quad (7)$$

In the present study the F atom yield in the low-pressure cell at full dose and 1000 mbar SF_6 was determined to be $(2.8 \pm 0.3) \times 10^{15}$ molecules cm^{-3}.

The F atom yield in the high-pressure cell was determined in a similar way. Mixtures of 50 mbar CH_4, 100 mbar at O_2, and 0–19.5 bar of SF_6 were radiolyzed by a 2 μs pulse of 10 MeV

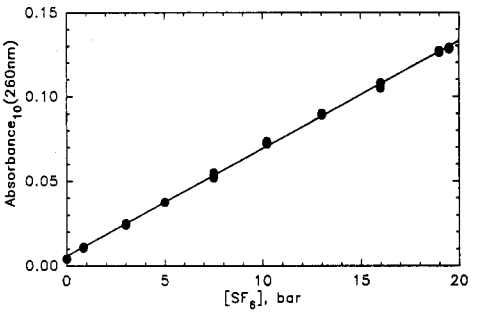

Figure 2. Transient absorption at 260 nm following pulse radiolysis of 50 mbar CH_4, 100 mbar O_2, and 0–19.5 bar of SF_6. The straight line is determined by linear regression of the data.

electrons. The absorbance due to CH_3O_2 radicals was measured at 260 nm as a function of the SF_6 pressure and is plotted in Figure 2. It is seen from the figure that the absorbance is proportional to the SF_6 concentration and thereby to the F atom concentration in the gas cell. By linear regression, the slope of the straight line in Figure 2 is determined to be $(6.36 \pm 0.08) \times 10^{-3}$ bar^{-1}. From this slope and the absorption cross section of the CH_3O_2 radical at 260 nm of 3.18×10^{-18} cm^2 molecule^{-1},[15] and taking into account a small correction due to the reaction of F atoms with O_2 (k_4 at 18 bar SF_6 is later determined to be 2.7×10^{-12} cm^3 molecule^{-1} s^{-1}), an estimate of the fluorine atom yield at 18 bar SF_6 of $(4.5 \pm 0.5) \times 10^{15}$ molecules cm^{-3} was derived. The uncertainty includes 10% uncertainty in σ_{CH3O2} (260 nm) and the uncertainty in the slope in Figure 2.

FO_2 radicals were generated in both setups by radiolysis of mixtures of O_2 and SF_6:

$$SF_6 + 2 \text{ or } 10 \text{ MeV } e^- \rightarrow F + \text{products} \quad (5)$$

$$F + O_2 + M \rightarrow FO_2 + M \quad (4)$$

The pseudo-second-order rate constant for reaction 4 is well-known at 1 bar of SF_6 total pressure, $k_4 = (1.9 \pm 0.3) \times 10^{-13}$ cm^3 molecule^{-1} s^{-1}.[9] SF_6 pressures were 1 bar (within 5%) in all experiments in the low-pressure cell. The SF_6 pressure applied in the high-pressure cell was 18 bar. k_4 at 18 bar SF_6 is determined later to be $(2.7 \pm 0.7) \times 10^{-12}$ cm^3 molecule^{-1} s^{-1}.

Reagents and concentrations used were as follows: SF_6 (>99.97%), 0.9–19 bar; CH_4 (>99%), 0–600 mbar; and CO (>99.9%), 0–500 mbar; O_2, ultrahigh purity, 50–1000 bar; NO (>99.8%), 0–0.65 mbar; and NO_2 (>98%), 0–3 mbar. SF_6, CH_4, and CO were supplied by Gerling and Holz. O_2 was supplied by L'Air Liquide. NO was obtained from Messer Griesheim, and NO_2 was supplied by Linde Techniche Gase. All reagents were used as received.

Ozone was produced by flowing O_2 through a conventional discharge ozonizer. The O_2 was purified before it entered the ozonizer by flowing it through a silica gel trap. The ozone/oxygen mixture was flowed through a silica gel trap cooled to −78 °C by an ethanol and dry ice bath. After ozone was collected on the silica gel trap for 3 h, the silica gel trap with ozone was hooked directly to the gas inlet on the high-pressure cell. The ozone/oxygen gas mixture in the silica gel trap flowed directly into the cell. Ozone concentrations were determined by measurements of the absorption at 220 or 288 nm in the cell before and after the gas cell was filled with the ozone/oxygen mixture. The ozone absorption cross sections used for quantifications of ozone were 1.80×10^{-18} cm^2 at 220 nm and 1.79×10^{-18} cm^2 at 288 nm.[16] Ozone concentrations were in the range 0–4 mbar.

Results

The reactions of the FO_2 radical with NO and NO_2 were investigated using the low-pressure cell. The rate constant of the

reaction of FO_2 with NO was determined from the formation kinetics of FNO at 310.5 nm. The rate constant of the reaction between FO_2 and NO_2 was determined by the decays of NO_2 at 400 nm and FO_2 at 220 nm.

The high-pressure cell was used to study the reactions of FO_2 with NO_2, O_3, CH_4, and CO. Performing the experiments in the high-pressure cell had two advantages: (i) high O_2 concentrations could be used, and (ii) k_4 is greater at the high total pressures that could be used in this cell. Therefore it was easier to avoid the reaction of F atoms with the reactant species CH_4, NO_2, O_3, and CO. As a preliminary exercise, the rate of the reaction of F atoms with O_2 at 18 bar SF_6 was determined by a relative rate technique. To determine the rate constants of the reactions of FO_2 radicals with NO_2, O_3, CO, and CH_4, the decay of FO_2 was followed at 220 nm.

It is important in both systems to work under conditions where the initially formed F atoms react mainly with O_2 and not with the species X we have added to the reaction mixture to study the reaction between FO_2 and X:

$$F + O_2 + M \rightarrow FO_2 + M \quad (4)$$

$$F + X \rightarrow \text{products} \quad (8)$$

$$FO_2 + X \rightarrow \text{products} \quad (9)$$

It is therefore necessary to know the reactivity of F atoms toward O_2 and the substance X to evaluate this potential complication. The percentage of F atoms reacting with X may be calculated from eq I:

$$\text{importance of reaction 8} = 100\% k_8[X]/(k_8[X] + k_4[O_2]) \quad (I)$$

The influence of reaction 8 can be calculated from k_8, k_4, and the concentrations of X and O_2.

Another possible complication is the decomposition of FO_2 producing F atoms which might react with the species X:

$$FO_2 + M \rightarrow F + O_2 + M \quad (-4)$$

$$F + O_2 + M \rightarrow FO_2 + M \quad (4)$$

$$F + X \rightarrow \text{products} \quad (8)$$

The rate constant of reaction 4 has been measured previously at 1 bar SF_6 to be $k_4 = (1.9 \pm 0.3) \times 10^{-13}$ cm^3 molecule^{-1} s^{-1}.[9] In the following, the rate constant at 18 bar SF_6 has been determined as $(2.7 \pm 0.7) \times 10^{-12}$ cm^3 molecule^{-1} s^{-1}. From these two values and the equilibrium constant for reaction 4, $K_p(295K) = 8.9 \times 10^{-16}$ cm^3 molecule^{-1},[10] values of k_{-4} at 1 bar SF_6 and 18 bar SF_6 of 213 and 3027 s^{-1} are derived. All studies of K_p indicate it is pressure independent.

We can now determine the rate of decay of FO_2 in the presence of a substance X if FO_2 does not react with X via reaction 9 but F atoms react with X via reaction 8. If all F atoms produced by the decomposition of FO_2 react with X, the decay of FO_2 would be equal to k_{-4}. However, only a fraction of the F atoms react with X in competition with O_2. This fraction is given by the equation $k_8[X]/(k_8[X] + k_4[O_2])$. The first-order decay rate coefficient is then

$$k_{decay} = k_{-4}k_8[X]/(k_8[X] + k_4[O_2]) \quad (II)$$

In the experiments reported in the present study we have used conditions where $k_8[X] \ll k_4[O_2]$. Therefore k_{decay} can be written:

$$k_{decay} \approx k_8[X]/K_p[O_2] \quad (III)$$

TABLE 1: Comparison of Measured Rate Constants and $k_{decay}/[X]$

compd X	exp rate, 10^{-16} cm^3 molecule^{-1} s^{-1}	k_8, 10^{-11} cm^3 molecule^{-1} s^{-1}	$k_{decay}/[X]$,[a] 10^{-16} cm^3 molecule^{-1} s^{-1}
O_3[b]	2.8 ± 0.6	1.0[3,23]	4.6
CH_4[b]	36 ± 5	6.8[19]	31
CO[b]	4.8 ± 0.3	1.2[d]	5.5
NO_2[b]	$(1.0 \pm 0.1) \times 10^3$	3.0[16]	14
NO_2[c]	$(1.1 \pm 0.1) \times 10^3$	3.0[16]	14
NO[c]	$(1.5 \pm 0.1) \times 10^4$	0.5[13]	2.3

[a] $k_{decay}/[X] = k_8/K_p[O_2]$. [b] High-pressure cell. [c] Low-pressure cell. [d] This work.

k_{decay} is the first-order decay rate coefficient of FO_2 radicals in the presence of X if the FO_2 radical does not react with X. $k_{decay}/[X]$ will then be the rate constant for the decay of the FO_2 even though FO_2 radicals do not react with the species X. $k_{decay}/[X]$ is the lowest possible result of a measurement of k_9. In Table 1 we have listed values of k_9 and $k_{decay}/[X]$. By comparison of the experimentally measured value of k_9 with the values of $k_{decay}/[X]$ given in Table 1 we can determine whether the measured rate constant is a real k_9 or just the result of the reaction mechanism, k_4, k_{-4}, and k_8. The results are discussed in the paragraphs dealing with the specific reactions.

Rate Constant for the Reaction of FO_2 Radicals with NO. In the low-pressure cell, radiolysis of 50 mbar O_2, 0.21–0.65 mbar NO, and 1000 mbar SF_6 was used to study the reaction between the FO_2 radical and NO. This reaction has two possible reaction pathways:

$$FO_2 + NO \rightarrow FNO + O_2 \quad (10a)$$

$$FO_2 + NO \rightarrow FO + NO_2 \quad (10b)$$

Reaction 10a is 43.6 kcal mol^{-1} exothermic[16] while reaction 10b is 6 kcal mol^{-1} endothermic.[16] To evaluate the branching of reaction 10, the yield of FNO was determined by the absorption at 310.5 nm. The transient absorbance at 310.5 nm following radiolysis of a mixture of 0.44 mbar NO, 50 mbar O_2, and 1000 mbar SF_6 is shown in Figure 3A. The average absorbance of the six recorded FNO transients was 0.044 ± 0.006. Using σ_{FNO}(310.5 nm) = 5.7×10^{-19} cm^2 molecule^{-1},[17] path length = 120 cm, dose 0.527, and an F atom yield at full dose and 1000 mbar of SF_6 of $(2.8 \pm 0.3) \times 10^{15}$ molecule cm^{-3}, we obtain a yield of FNO of $100 \pm 14\%$. Clearly, a is the major reaction channel for reaction 10. Channel 10a could proceed through a 4-center rearrangement.

The rate of reaction 10 was determined by fitting a first-order rise expression to the formation of FNO at 310.5 nm. The transients were always fitted well by a first-order expression. The pseudo-first-order rates obtained in this way are plotted in Figure 4 as a function of the NO concentration. The slope of a straight line through the data points gives $k_{10} = (1.5 \pm 0.1) \times 10^{-12}$ cm^3 molecule^{-1} s^{-1}.

Rate Constant for the Reaction of FO_2 Radicals with NO_2 Using the Low-Pressure Cell. The rate constant for the reaction of FO_2 with NO_2 was determined by monitoring the decay of NO_2 and FO_2 following radiolysis of 0.3–3.0 mbar NO_2, 50 mbar of O_2, and 1000 mbar of SF_6:

$$FO_2 + NO_2 \rightarrow \text{products} \quad (11)$$

The final absorption in Figure 3B is less than that before the radiolysis pulse. This is not surprising since the absorption at 220 nm is a combination of that from FO_2 radicals and NO_2. NO_2 is consumed by reaction 11, leading to a final absorbance which is less than that observed before the radiolysis pulse. As seen from Figure 3C, the transient absorption observed at 400 nm has an interesting shape. The absorption at 400 nm is due solely to NO_2. The large initial drop in absorption is caused by

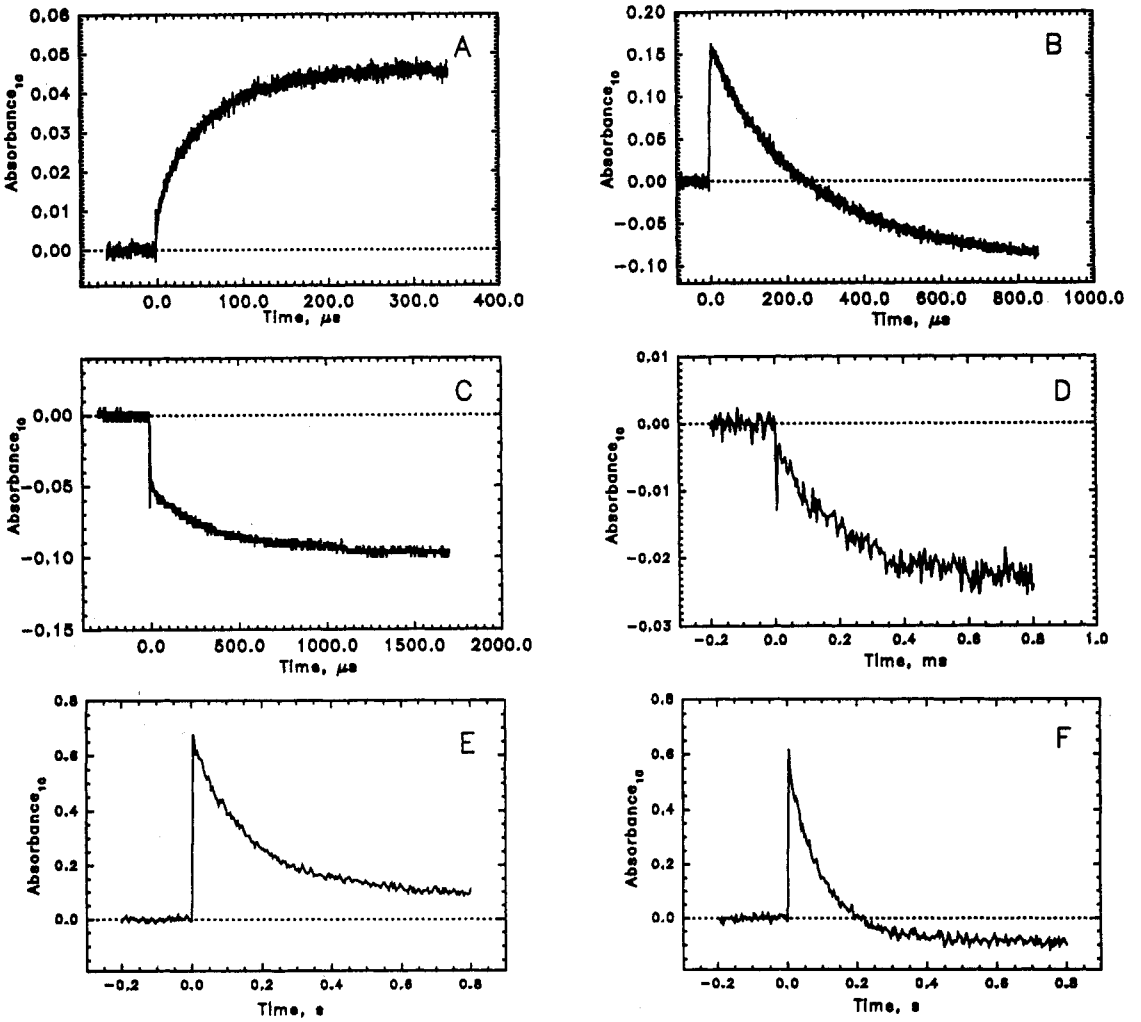

Figure 3. Transient absorptions observed at the following wavelengths and conditions: (A) at 310.5 nm with 0.44 mbar NO, 50 mbar O_2, and 950 mbar SF_6; (B) at 220 nm with 1.0 mbar NO_2, 50 mbar of O_2, and 950 mbar of SF_6; (C) at 400 nm with 0.5 mbar NO_2, 50 mbar of O_2, and 950 mbar of SF_6; (D) at 400 nm with 2 mbar NO_2, 1000 mbar O_2, and 18 bar SF_6; (E) at 220 nm with 1000 mbar O_2 and 18 bar SF_6; (F) at 220 nm with 1.3 mbar O_3, 1000 mbar O_2, and 18 bar SF_6.

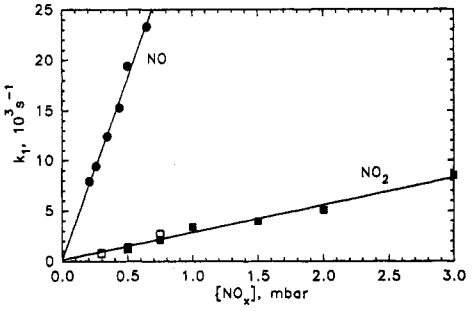

Figure 4. First-order formation rates of FNO at 310.5 nm (●) and first-order decay rates of FO_2 at 220 nm (■) and NO_2 at 400 nm (□). The straight lines are found by linear regressions of the data.

the scavenging of some of the F atoms by NO_2. The subsequent decay is caused by the reaction of FO_2 radicals with NO_2. In considering the transient in Figure 3C, it should be noted that the observed change in absorption represents only a small fraction (<20%) of the total absorption at this wavelength.

Pseudo-first-order decay rate constants obtained from traces such as those shown in Figure 3B and 3C are plotted as a function of the NO_2 concentration in Figure 4. As seen in Figure 4, the kinetic data obtained by monitoring the decay of absorption at 220 and 400 nm were in good agreement. A linear regression of the data in Figure 4 gives $k_{11} = (1.1 \pm 0.1) \times 10^{-13}$ cm^3 molecule^{-1} s^{-1}. The products of reaction 11 are unknown. Reaction 11 may proceed via a mechanism involving a 4-center rearrangement to give FNO_2 and O_2. Alternatively, reaction 11 may proceed to give the adduct FO_2NO_2.

At this point we need to consider potential complications in our measurement of k_{11}. One complication could be the formation of FNO_2 via reaction 11 or via the direct reaction of F atoms with NO_2 (as evidenced by the initial drop in absorption seen in Figure 3C). FNO_2 is a stable compound which absorbs only weakly in the UV (σ(max) = 2.6×10^{-20} cm^2 molecule^{-1} at 230 nm[18]). The formation of FNO_2 is not expected to complicate the present kinetic analysis. In light of the excellent agreement in the kinetic data derived using the two different wavelengths (220 and 400 nm) shown in Figure 4, it seems unlikely that the present work is subject to significant complications caused by unwanted radical species.

The Reaction of F Atoms with O_2 at 18 bar SF_6. At a pressure of 18 bar of SF_6 the rate constant for reaction 4 is expected to be significantly elevated as compared to k_4 at 1 bar SF_6 since the pseudo-second-order rate constant, k_4, is pressure dependent up to pressures higher than 1000 bar of He.[10] Therefore we have measured k_4 at 18 bar of SF_6.

It was not possible to measure k_4 directly by the 220 nm absorption of FO_2 that is formed in the reaction. At the low oxygen concentrations necessary to measure the formation kinetics, radical–radical reactions such as the reaction of F atoms with the FO_2 radical become important. This increases the apparent formation kinetics of FO_2 so much that it was impossible to derive a meaningful reaction rate from direct measurements. Therefore a relative rate method was applied.

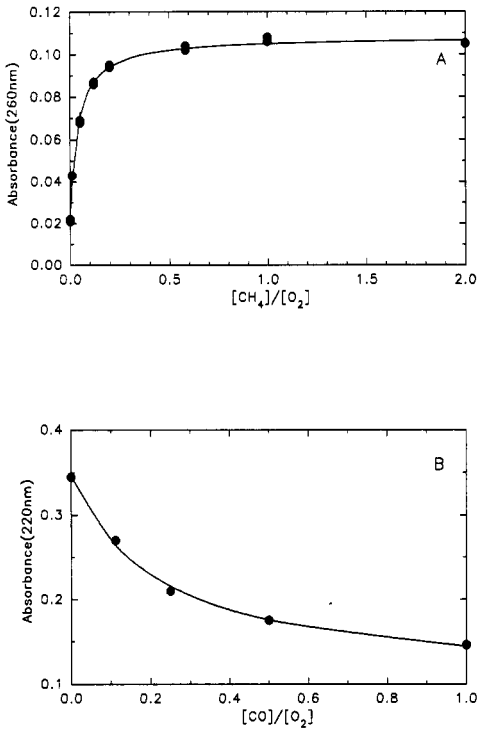

Figure 5. (A) Maximum transient absorbance at 260 nm following pulse radiolysis of 0–600 mbar CH_4, 300–1000 mbar O_2, and 18 bar SF_6 as a function of the concentration ratio $[CH_4]/[O_2]$. (B) Maximum transient absorbance at 220 nm following pulse radiolysis of 0–500 mbar CO, 500–1000 mbar O_2, and 18 bar SF_6 as a function of the concentration ratio $[CO]/[O_2]$. Solid lines are fits to the data; see text.

The pseudo-second-order rate constant, k_4, at 18 bar SF_6 was determined relative to the rate constant for reaction of F atoms with CH_4, k_6. The literature data on the reactivity of F atoms toward methane are discussed by Wallington et al.,[19] and a value of $(6.8 \pm 1.4) \times 10^{-11}$ cm^3 molecule^{-1} s^{-1} was derived. This rate constant is not pressure dependent.

When mixtures of $O_2/CH_4/SF_6$ are radiolyzed, FO_2 and CH_3O_2 are formed from the following set of reactions:

$$SF_6 + 10\ \text{MeV}\ e^- \rightarrow F + \text{products} \quad (5)$$

$$F + O_2 + M \rightarrow FO_2 + M \quad (4)$$

$$F + CH_4 \rightarrow CH_3 + HF \quad (6)$$

$$CH_3 + O_2 + M \rightarrow CH_3O_2 + M \quad (7)$$

The amounts of FO_2 radicals relative to the amount of CH_3O_2 radicals formed depends only on the ratio between the rate constant of F atom reactions with CH_4 and O_2, k_6/k_4, and the ratio between the methane concentration and the oxygen concentration, $[CH_4]/[O_2]$.

As a measure of the CH_3O_2 concentration, the absorbance at 260 nm following pulse radiolysis of mixtures of 300–500 mbar of O_2, 0–600 mbar CH_4, and 18 bar SF_6 was used. In these experiments the radiolysis time of 2 μs and a SF_6 concentration of 18 bar were held constant ($[F]_0 = 4.5 \times 10^{15}$ molecules cm^{-3}).

Figure 5A shows the observed variation of the maximum transient absorption as function of the concentration ratio $[CH_4]/[O_2]$. As seen from this figure, the absorbance at low $[CH_4]/[O_2]$ ratio was small, around 0.02. As the concentration ratio increased, the absorption increased until a ratio $[CH_4]/[O_2]$ of 1 was reached. Further increase in the ratio $[CH_4]/[O_2]$ had no discernible effect on the absorption. This behavior is rationalized in terms of the competition between CH_4 and O_2 for the available F atoms. At low CH_4 concentrations, an appreciable amount of FO_2 is formed; hence, a small initial absorption at 260 nm is seen. As the CH_4 concentration is increased, an increasing fraction of the F atoms reacts with CH_4 at the expense of O_2, and the initial maximum absorption increases.

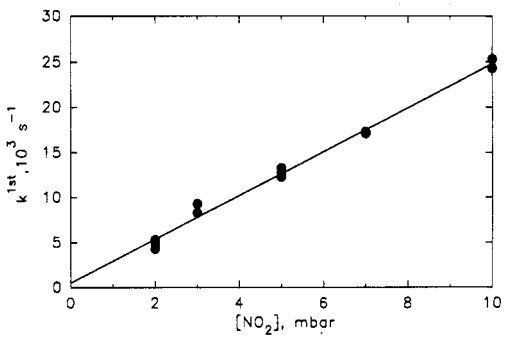

Figure 6. First-order decay rates of NO_2 measured at 400 nm following pulse radiolysis of 2–10 mbar NO_2, 1000 mbar O_2, and 18 bar SF_6 plotted as a function of $[NO_2]$. The solid line is a linear regression of the data.

The solid line in Figure 5A represents a three-parameter fit of the following expression to the data:

$$A_{max} = \{A_{FO2} + (A_{CH3O2}(k_6/k_4)[CH_4]/[O_2])/(1 + (k_6/k_4)[CH_4]/[O_2])\} \quad (IV)$$

where A_{max} is the observed maximum transient absorbance, A_{FO2} is the maximum absorbance expected if only FO_2 is produced, and A_{CH3O2} is the maximum absorbance expected if all F atoms react with CH_4. Parameters A_{FO2}, A_{CH3O2}, and k_6/k_4 were simultaneously varied. The best fit was obtained with $k_6/k_4 = 25.1 \pm 3.4$, $A_{FO2} = 0.023 \pm 0.003$, and $A_{CH3O2} = 0.108 \pm 0.018$. Errors are two standard deviations. Using our value of $k_6 = (6.8 \pm 1.4) \times 10^{-11}$ cm^3 molecule^{-1} s^{-1}, k_4 is $(2.7 \pm 0.7) \times 10^{-12}$ cm^3 molecule^{-1} s^{-1} (quoted errors reflect uncertainty in k_6 and the ratio k_6/k_4). This is concluded to be the pseudo-second-order rate constant for the reaction of F atoms with O_2 at 18 bar SF_6.

Rate Constant for the Reaction of FO_2 Radicals with NO_2 Using the High-Pressure Cell. The decay of NO_2 was used to study the reaction between FO_2 and NO_2 in the high-pressure cell. These experiments were performed to verify the result from the low-pressure cell and to check for any pressure dependence of the reaction between FO_2 and NO_2. The pseudo-first-order rate constant for the reaction of FO_2 with NO_2 was derived by observing the decay of NO_2 and by plotting $\ln\{(Abs_t - Abs_\infty)/Abs_t\}$ against the time. Abs_t and Abs_∞ are the absorbances at time t and $t = \infty$, respectively. If the reaction is first order, then a plot of $\ln\{(Abs_t - Abs_\infty)/Abs_t\}$ versus time gives a straight line with a slope of the pseudo-first-order rate constant. Following radiolysis of 2 mbar NO_2, 1000 mbar O_2, and 18 bar SF_6, the transient absorbance observed at 400 nm is displayed in Figure 3D. The pseudo-first-order rates found from the experimental transients at 400 nm as described above are plotted as a function of $[NO_2]$ in Figure 6. A linear regression of the data gives a rate constant of $(1.05 \pm 0.10) \times 10^{-13}$ cm^3 molecule^{-1} s^{-1}. It should be noted that the same value of k_{11} is obtained by both the high- and the low-pressure techniques. Reaction 11 shows no pressure dependence in the range of 1–18 bar SF_6.

It is expected that the products of the reaction of FO_2 with NO_2 are either FO_2NO_2 or FNO_2 and O_2. Formation of FO and NO_3 is not feasible since this reaction is 29 kcal mol^{-1} endothermic.[16] The two first mentioned product channels give stable products, and it is therefore not expected that these products change the apparent decay of NO_2. Hence, we do not expect any interference with secondary chemistry on the experimental data.

As seen from Table 1, $k_{decay}/[NO_2] \ll k_{11}$, so the interference from the direct reaction of F atoms with NO_2 is negligible. We choose to quote a value for k_{11} of $(1.05 \pm 0.10) \times 10^{-13}$ cm^3 molecule^{-1} s^{-1} from the present work.

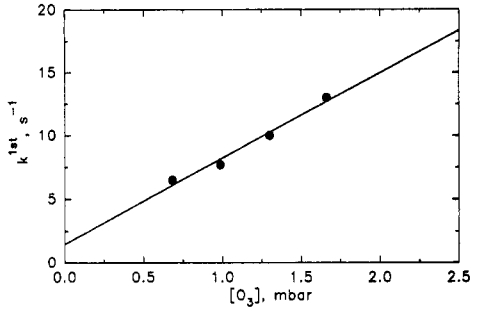

Figure 7. First-order decay rates of FO_2 measured at 220 nm following pulse radiolysis of 0.65–1.7 mbar O_3, 1000 mbar O_2, and 18 bar SF_6 plotted as a function of $[O_3]$. The solid line is a linear regression fit of the data.

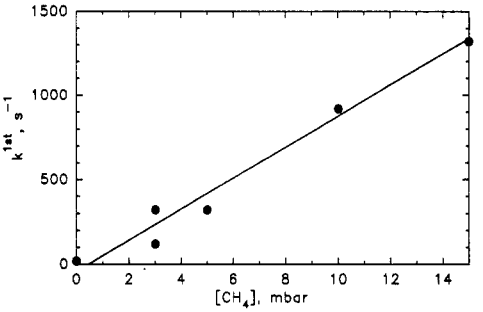

Figure 8. First-order decay rates of FO_2 measured at 220 nm following pulse radiolysis of 0–15 mbar CH_4, 1000 mbar O_2, and 18 bar SF_6 plotted as a function of $[CH_4]$. The solid line is a linear regression fit of the data.

The Reaction of FO_2 with O_3. Displayed in Figure 3E and 3F are two FO_2 transients recorded at 220 nm without and with 1.3 mbar of ozone, respectively. It is seen from the figure that small amounts of ozone increase the apparent decay of FO_2. Pseudo-first-order decay rates were determined from the slope of a plot of $\ln\{(Abs_t - Abs_\infty)/Abs_t\}$ versus time as described above. The rates are plotted in Figure 7 against the ozone concentration. The slope found by linear regression of the data gives a reaction rate of $(2.8 \pm 0.6) \times 10^{-16}$ cm^3 molecule^{-1} s^{-1}. The plot in Figure 7 has a significant intercept, 1.5 ± 1.4 s^{-1}. This intercept corresponds to the decay of the FO_2 radicals in the cell without any other substances present.

As shown in Table 1, $k_{decay}/[O_3]$ is close to the value found for the rate constant of the reaction of FO_2 with ozone. Hence, within the uncertainty, the FO_2 radicals do not react with ozone and an upper limit of 3.4×10^{-16} cm^3 molecule^{-1} s^{-1} can be derived from the data.

As an additional check on the system, the behavior of ozone was recorded by measuring the absorbance at 288 nm. A loss of ozone was observed. This may be explained by the reaction of F atoms, formed in the decomposition of the FO_2 radical, with ozone:

$$FO_2 + M \rightarrow F + O_2 + M \qquad (-4)$$

$$F + O_3 \rightarrow FO + O_2 \qquad (12)$$

The loss of ozone was in all cases $100 \pm 16\%$ of the initial F atom yield including an uncertainty of 10% in the F atom calibration. The upper limit of the ozone loss of 116% gives us an upper limit for the reaction of FO with ozone,

$$FO + O_3 \rightarrow FO_2 + O_2 \qquad (1)$$

because if this reaction were fast the result would be more than 100% ozone loss. The highest ozone concentration used in the present work was 4 mbar. At this ozone concentration the decay of the 4.5×10^{15} molecule cm^{-3} FO_2 radicals will produce almost the same amount of FO radicals by decomposition of FO_2 followed by reaction of F atoms with ozone. A maximum of 16% of these FO radicals will react with ozone. The other 84% will be consumed by some other loss reactions. The fastest possible loss reaction of FO radicals apart from reaction with O_3 is the reaction with FO_2:

$$FO + FO_2 \rightarrow \text{products} \qquad (13)$$

The maximum rate constant for this reaction is the diffusion limit, about 10^{-10} cm^3 molecule^{-1} s^{-1}. This reaction will, however, reduce the amount of FO radicals formed to half of the amount of FO_2 radicals formed. Therefore, up to 32% of the FO radicals may react with ozone. This gives us the following equation:

$$k_1[O_3]/(k_1[O_3] + k_{13}[FO_2]) = 1/(1 + k_{13}[FO_2]/(k_1[O_3])) < 0.32 \quad (V)$$

Using $k_{13} = 10^{-10}$ cm^3 molecule^{-1}, $[FO_2] = 0.2$ mbar, and $[O_3] = 4$ mbar,

$$1/(1 + 5 \times 10^{-12}/k_1) < 0.32 \Leftrightarrow k_1 < 1.2 \times 10^{-12}$$

The upper limit for k_1 at 295 K is therefore 1.2×10^{-12} cm^3 molecule^{-1} s^{-1}. Recently, Bedzhanyan et al.[20] reported an upper limit for reaction 1 of 2×10^{-16} cm^3 molecule^{-1} s^{-1}.

The Reaction of FO_2 with CH_4. The reaction of FO_2 radicals with methane was studied using the decay of the FO_2 radical by following the transient absorption at 220 nm. An initial rate method was applied for this study: 0–15 mbar CH_4, 1000 mbar O_2, and 18 bar SF_6 were used. The initial rates of FO_2 loss at different methane concentrations divided by the initial FO_2 radical concentration gives the pseudo-first-order rate constants. These are plotted as a function of $[CH_4]$ in Figure 8. The slope of a straight line through the data gives a rate constant of $(3.6 \pm 0.5) \times 10^{-15}$ cm^3 molecule^{-1} s^{-1}. As seen in Table 1, this value is similar to $k_{decay}/[CH_4]$, indicating that the determined value is not a "true" rate constant for the reaction of the FO_2 radical with CH_4 but rather an upper limit.

Possible complications of the measurement above included (i) reactions of products of the methane degradation with FO_2 and (ii) reaction of F atoms formed initially with CH_4. The first complication cannot be ruled out but probably is not a serious complication since FO_2 radicals seem to react slowly with most species. However, if this reaction is important, it will tend to speed the decay of the FO_2 radicals; hence the upper limit above is still valid. The second complication will also tend to increase the apparent decay at 220 nm since the decay of CH_3O_2 is faster than that of FO_2. Using $k_4 = 2.7 \times 10^{-12}$ cm^3 molecule^{-1} s^{-1} and $k_6 = 6.8 \times 10^{-11}$ cm^3 molecule^{-1} s^{-1}, we calculate for the highest methane concentration used a yield of 27% of initially formed CH_3 radicals by direct reaction of the initially formed F atoms with CH_4. This will, as stated previously, increase the apparent decay rate at 220 nm, and hence the upper limit is still valid.

The Reaction of FO_2 with CO. The reaction of FO_2 with CO was studied by monitoring the FO_2 decay at 220 nm. In a set of preliminary experiments, the rate of reaction of F atoms with CO was measured at 18 bar SF_6. The maximum transient absorbance at 220 nm was measured following radiolysis of 0–500 mbar CO, 500–1000 mbar O_2, and 18 bar SF_6. The absorbance data are shown as a function of $[CO]/[O_2]$ in Figure 5B. In the system, CO and O_2 compete for the available F atoms in the two reactions

$$F + CO + M \rightarrow FCO + M \qquad (14)$$

$$F + O_2 + M \rightarrow FO_2 + M \qquad (4)$$

FCO radicals react rapidly with O_2 to give $FC(O)O_2$:[13]

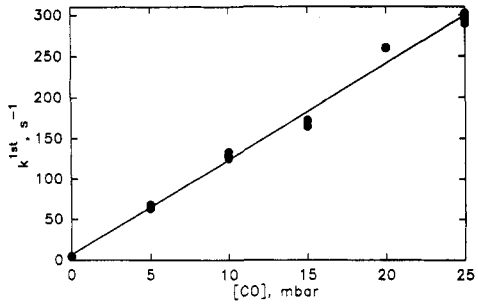

Figure 9. First-order decay rates of FO_2 measured at 220 nm following pulse radiolysis of 0–25 mbar CO, 1000 mbar O_2, and 18 bar SF_6 plotted as a function of [CO]. The solid line is a linear regression fit of the data.

$$FCO + O_2 + M \rightarrow FC(O)O_2 + M \qquad (15)$$

The absorbance at 220 nm is therefore a combination of the absorbances of FO_2 and $FC(O)O_2$. At low CO concentrations the absorbance at 220 nm is mainly due to FO_2. As the concentration of CO is increased, more and more $FC(O)O_2$ is formed relative to FO_2. We can now rationalize the absorbance behavior in Figure 5B since the absorption cross section of FO_2 at 220 nm is larger than that of $FC(O)O_2$.[13] By analogy with the determination of k_4, the data in Figure 5B may be fitted by the following expression:

$$A_{max} = \{A_{FO2} + (A_{FC(O)O2}(k_{14}/k_4)[CO]/[O_2])/(1 + (k_{14}/k_4)[CO]/[O_2])\} \qquad (VI)$$

where A_{FO2} and $A_{FC(O)O2}$ are the absorbances if all F atoms were converted into FO_2 or $FC(O)O_2$ radicals, respectively. A three-parameter fit of A_{FO2}, $A_{FC(O)O2}$, and k_{14}/k_4 gave a ratio between the two rate constants of 4.5 ■ 1.4. The fit may be seen as the solid line in Figure 5B. Using $k_4 = (2.7 \pm 0.7) \times 10^{-12}$ cm^3 molecule^{-1} s^{-1}, we derive $k_{14} = (1.2 \pm 0.5) \times 10^{-11}$ cm^3 molecule^{-1} s^{-1}; the quoted error reflects the cumulative uncertainties in the measured ratio k_{14}/k_4 and k_4.

In the following, concentration ratios $[CO]/[O_2]$ of up to 0.025 were used to determine the rate constant for the reaction of FO_2 with CO. Using $k_{14}/k_4 = 4.5$, we discover that the amount of initially formed $FC(O)O_2$ is less than 10% of the initial amount of F atoms formed in the system.

To measure the rate constant for the reaction of FO_2 radicals with CO, mixtures of 0–25 mbar CO, 1000 mbar O_2, and 18 bar SF_6 were radiolyzed, and the first-order rate of decay of the absorption at 220 nm was determined. The first-order decay rates were determined from the slope of a plot of $\ln\{(Abs_t - Abs_\infty)/Abs_i\}$ versus time, as described above. The first-order rates are plotted against [CO] in Figure 9. The slope found by linear regression of the data gives a rate constant for the reaction of FO_2 with CO of $(4.8 \pm 0.3) \times 10^{-16}$ cm^3 molecule^{-1} s^{-1}.

This rate constant may be influenced by reactions of FO_2 with $FC(O)O_2$ and other CO degradation products. However, it is seen from this work that the FO_2 radical is very unreactive, so it seems likely that the kinetics of the FO_2 radical are not significantly perturbated by the degradation products. As seen in Table 1, the measured rate constant for the reaction of FO_2 with CO is equal to $k_{decay}/[CO]$. This indicates that the reaction rate of FO_2 with CO may be zero within the uncertainty of the experiment. The value of $(4.8 \pm 0.3) \times 10^{-16}$ cm^3 molecule^{-1} s^{-1} is therefore an upper limit.

Discussion

As seen from the results of this work, FO_2 reactions are generally very slow. There are two possible reaction pathways of the reaction of FO_2 radicals with the species X: (i) Reactions where the F atom is the active part of the FO_2 radical. For example in the reaction with NO, >86% of the products were FNO and O_2, probably formed via the reaction complex ON–FO_2; (ii) reactions where the O–O• moiety of the FO_2 radical is the active part (i.e. where FO_2 reacts as a peroxy radical). We have not detected any evidence for peroxy radical type behavior for FO_2.

Reaction channel i is expected to be slow because of the large activation energy involved in the abstraction of an F atom from the FO_2 radical (~12.6 kcal mol^{-1}).[7] However, if the species X is capable of forming a low-energy reaction complex where the activation barrier is lowered effectively, a reaction is possible. It seems likely that NO is capable of doing this, while CH_4 does not effectively lower the activation barrier. A study of the temperature dependence of the reaction of FO_2 with NO and NO_2 would be of interest in this connection.

The FO_2 radical also seems very unreactive through reaction channel ii. As stated above, no experimental evidence for this reaction pathway was found in this work. No rates have been measured for reactions of FO_2 with other peroxy radicals. However, FO_2 seems stable in the presence of other peroxy radicals.[21] The conclusion is that FO_2 is not a very reactive radical.

Atmospheric Implications. The known reactions of F, FO, and FO_2 of importance in the atmosphere are displayed in Table 2. Apart from the unimolecular decomposition of the FO_2 radical, all known activation energies are small. The rate constants at 295 and 220 K differ by less than a factor of 2. For simplicity we have therefore only considered the temperature dependence of the self-decomposition of the FO_2 radicals in the following. While the temperature dependences of the rate constants of the first five reactions in Table 2 are not known, it is expected that the rates of these reactions will slow down at lower temperatures because of the significant energy involved in abstraction of F atoms from the FO_2 radical.

To evaluate the importance of the reactions of the F, FO, and FO_2 radicals in the atmosphere, knowledge of the atmospheric concentrations of the reactants is necessary. We have used known values of NO, NO_2, CO, O_3, O, and M and the temperature from Brasseur and Solomon.[22] These are known concentrations at mid latitudes. Figure 10A–C shows the lifetimes of F atoms (Figure 10A), FO radicals (Figure 10B), and FO_2 radicals (Figure 10C) with respect to reactions with atmospheric-important species at different altitudes. There are reactions in Table 2 which directly or indirectly destroy odd oxygen (O atoms or O_3 molecules):

$$F + O_3 \rightarrow FO + O_2 \qquad (12)$$

$$FO + O_3 \rightarrow FO_2 + O_2 \qquad (1)$$

TABLE 2: FO_x Reactions

reaction	rate constant (295 K), cm^3 molecule^{-1} s^{-1}	ref
$FO_2 + NO \rightarrow FNO + O_2$	$(1.5 \pm 0.1) \times 10^{-12}$	this work
$FO_2 + O_3 \rightarrow FO + 2O_2$	$<3.4 \times 10^{-16}$	this work
$FO_2 + NO_2 \rightarrow$ products	$(1.05 \pm 0.10) \times 10^{-13}$	this work
$FO_2 + CO \rightarrow$ products	$<5.1 \times 10^{-16}$	this work
$FO_2 + CH_4 \rightarrow$ products	$<4.1 \times 10^{-15}$	this work
$FO_2 + M \rightarrow F + O_2 + M$	3.75×10^{-8}[M] exp(−6711/T)[b]	10,7
$FO_2 + O \rightarrow FO + O_2$	5.0×10^{-11}[a]	16
$FO + NO \rightarrow NO_2 + F$	2.6×10^{-11}	16
$FO + O \rightarrow F + O_2$	2.7×10^{-11}	20
$FO + O_3 \rightarrow$ products	$<2 \times 10^{-16}$	20
$FO + O_3 \rightarrow$ products	$<1.2 \times 10^{-12}$	this work
$FO + ClO \rightarrow F + Cl + O_2$	5×10^{-11}	c
$F + CH_4 \rightarrow CH_3 + HF$	$(6.8 \pm 1.4) \times 10^{-11}$	19
$F + H_2O \rightarrow OH + HF$	1.4×10^{-11}	16
$F + O_3 \rightarrow FO + O_2$	1.0×10^{-11}	3,23
$F + O_2 + M \rightarrow FO_2 + M$	4.4×10^{-33}[M]	7

[a] Uncertain, no experimental data. [b] Calculated from $k_{-4} = k_4/K_d$. k_4 is taken from ref 7 and K_d from ref 10. [c] Rate and products found by analogy to other halogen oxide self-reactions.

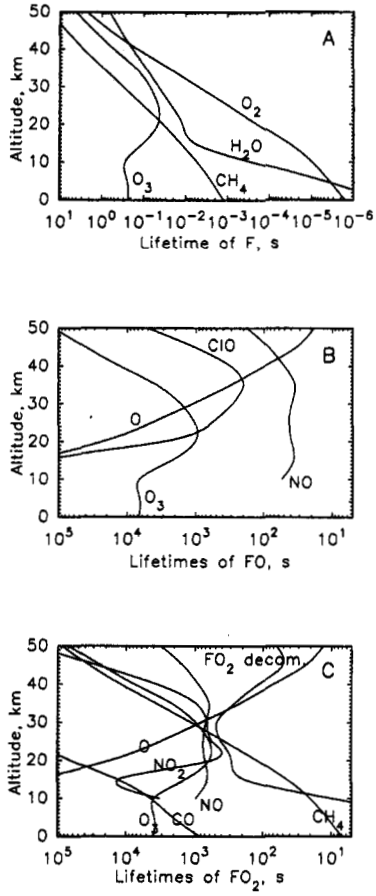

Figure 10. Lifetimes, $t = 1/(k_{FO_x+X}[X])$, of F atoms (A), FO radicals (B), and FO_2 radicals (C) with respect to reaction with atmospheric-important species at different altitudes. The concentrations are taken from Brasseur and Solomon[22] and the rate constants from Table 2.

$$FO + O \rightarrow F + O_2 \qquad (16)$$

$$FO + ClO \rightarrow F + Cl + O_2 \qquad (17)$$

$$FO_2 + O_3 \rightarrow FO + 2O_2 \qquad (3)$$

$$FO_2 + O \rightarrow FO + O_2 \qquad (2)$$

There are two reactions which remove the F atoms efficiently from the FO_x catalytic cycle:

$$F + CH_4 \rightarrow HF + CH_3 \qquad (6)$$

$$F + H_2O \rightarrow HF + OH \qquad (18)$$

HF is unreactive in the stratosphere and is transported to the troposphere where it is incorporated into rain droplets and rained out.

In the following we will establish an upper limit for the number of ozone molecules destroyed by one F atom formed in the atmosphere. The mechanism we will use to evaluate this is shown in Figure 11. The main reaction of F atoms in the atmosphere is reaction with O_2 to form FO_2. F atoms are then reformed by unimolecular decomposition of FO_2. FO radicals may be formed from the reaction of FO_2 radicals with O atoms and O_3 molecules and by the reaction of F atoms with ozone. FO radicals reform F atoms or FO_2 radicals by reaction with NO, O atoms, ClO, or ozone. F atoms are removed from the cycle by reaction with CH_4 and H_2O.

The number of times FO_2 is reformed through equilibrium 4 before its removal by reaction with H_2O or CH_4 is

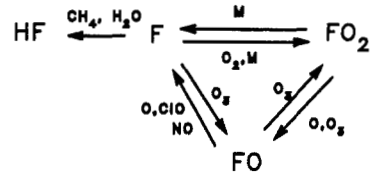

Figure 11. Reaction scheme of the kinetic model used in the calculation of the ozone destruction effectiveness of F atoms released to the stratosphere.

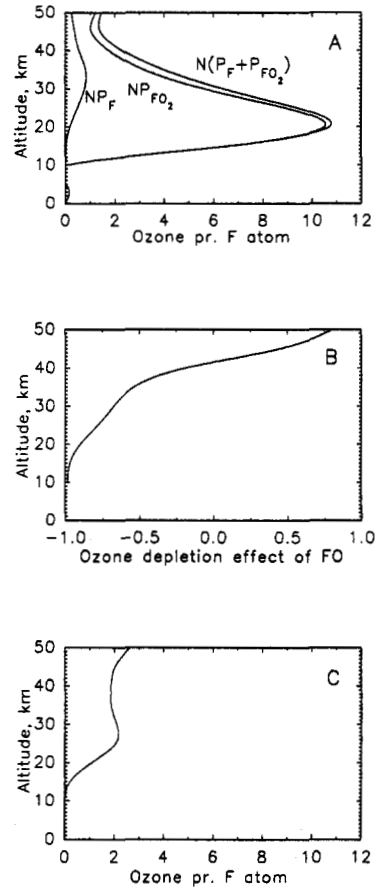

Figure 12. Plot of the number of ozone molecules destroyed by an F atom released to the stratosphere: simple model (A) and advanced model (C). Effect of an FO radical on the ozone layer before it forms FO_2 or F atoms (B). See text for details.

$$N = k_4[O_2]/(k_6[CH_4] + k_{18}[H_2O]) \qquad (VII)$$

The probability that FO_2 or F destroys an ozone molecule either as O_3 or O, before reaction with O_2 or decomposition, respectively, is

$$P_F = k_{12}[O_3]/k_4[O_2] \qquad (VIII)$$

$$P_{FO2} = (k_3[O_3] + k_2[O])/k_{-4} \qquad (IX)$$

Under the assumption that FO neither destroys nor forms ozone before it forms FO_2 radicals or F atoms, we can now derive an upper limit for the number of ozone molecules destroyed by one F atom released into the stratosphere. The upper limit is the product of the probability that FO_2 or F will destroy an ozone molecule before it is removed by decomposition or reaction with O_2, P_{FO2} or P_F, and the number of times F and FO_2 are reformed before F reacts with CH_4 or H_2O, $N(P_F + P_{FO2})$. NP_F, NP_{FO2}, and $N(P_F + P_{FO2})$ are plotted in Figure 12A at different altitudes. As seen from Figure 12A, the maximum number of ozone molecules destroyed per F atom formed in the stratosphere from this simple model is 11 at 20 km altitude.

Now we will make our model a little more sophisticated. We will consider the FO reactions and include a reaction which has an analog in ClO chemistry.

$$FO + ClO \rightarrow F + Cl + O_2 \quad (17)$$

This reaction could be fast with a rate constant of up to 5×10^{-11} cm^3 $molecule^{-1}$ s^{-1}. The lifetime of FO with respect to the reaction with ClO is plotted in Figure 10B. The maximum ozone destruction potential of a FO radical before it is converted into FO_2 or F atoms is determined by reaction with ClO, O atoms, O_2, and NO_2. FO destroys one ozone molecule before it forms F or FO_2 if it reacts with ClO, O_3, or O atoms. If it reacts with NO, it actually reforms an ozone molecule because the product, NO_2, photolyzes to give NO and an O atom. The effect of FO radicals on the stratospheric ozone layer may be calculated from

$$(k_{FO+NO}[NO] - k_{17}[ClO] - k_1[O_3] - k_{16}[O])/(k_{FO+NO}[NO] + k_{17}[ClO] + k_1[O_3] + k_{16}[O]) \quad (X)$$

The values determined by eq X at different altitudes are plotted in Figure 12B; −1 means that an ozone molecule is formed, by reaction with NO, before FO is converted into F atoms or FO_2 radicals, and +1 means that one ozone molecule is destroyed before FO is converted into FO_2 or F.

The real potential ozone destroying effect of the FO_x cycle may now be calculated as $N(P_F + P_{FO2})(1 + \text{FO effect})$ because every time a FO radical is produced an ozone molecule is lost and the effects of reforming F or FO_2 from FO may be calculated from eq V. As seen from Figure 12C, the maximum possible effect of the FO_x cycle is small. Less than about 2 ozone molecules are destroyed per F atom released into the stratosphere. This number should be compared to 10^3–10^4 for Cl atoms. The effect of F atoms on the stratospheric ozone layer is therefore likely to be negligible.

The method used to calculate the upper limit for the number of ozone molecules destroyed per F atom released into the stratosphere is not exact. However, it gives a good estimate of the ozone-depleting effect of F atoms and shows that, with the currently known FO_x reactions, FO_x cycles do not pose a threat to the stratospheric ozone layer.

From the discussion above we may now estimate an upper limit for the ODP (ozone depletion potential) of HFCs (hydrofluorocarbons) due to the ozone destruction by F atoms. Most HFCs have atmospheric lifetimes with respect to reaction with OH radicals of >5 years. Only 5–10% of the HFCs are degradated in the stratosphere, hence reducing the ODP of these compounds by a factor of at least 10 as compared to CFCs. As indicated above, F atoms are at least 1000 times less efficient than Cl atoms in destroying ozone in the stratosphere. An upper limit for the ozone depletion potential due to the FO_x cycles of HFC-134a (CF_3-CFH_2), an important CFC substitute, is $\sim 10^{-4}$. This value is determined under the worst case assumption that all the fluorine atoms in HFC-134a are released as F atoms. We therefore believe that the ozone depletion potential of HFCs due to F atoms formed in the stratosphere is negligible.

Acknowledgment. J.S. thanks the Danish Research Academy for a research scholarship. O.J.N. thanks the Commission of the European Communities for financial support. O.J.N. and J.S. thank, for financial support, the AFEAS under Contract CTR93-45/P93-120. The authors also thank Steve Japar (Ford Motor Co.) for helpful discussions. The authors are indebted to E. E. Larsen for the construction of the high-pressure gas cell and to T. Johansen for skillful operation of the linarc accelerator.

References and Notes

(1) Alternative Fluorocarbon Environmental Acceptability Study, W.M.O. Global Ozone Research and Monitoring Project, Report No. 20; Scientific Assessment of Stratospheric Ozone, Vol. 2, 1989.
(2) Scientific Assessment of Stratospheric Ozone Depletion: 1991, World Meteorological Organization Global Ozone Research and Monitoring Project, Report No. 25.
(3) Nielsen, O. J.; Sehested, J. *Chem. Phys. Lett.* **1993**, *213*, 433 and references therein.
(4) Ravishankara, A. R.; Turnipseed, A. A.; Jensen, N. R.; Barone, S.; Mills, M.; Howard, C. J.; Solomon, S. *Science* **1994**, *263*, 71.
(5) Francisco, J. S.; Su, Y. *Chem. Phys. Lett.* **1993**, *215*, 58.
(6) Francisco, J. S. *J. Phys. Chem.* **1993**, *98*, 2198.
(7) Pagsberg, P.; Ratajczak, E.; Sillesen, A.; Jodkowski, J. T. *Chem. Phys. Lett.* **1987**, *141*, 88.
(8) Lyman, J. L.; Holland, R. *J. Phys. Chem.* **1988**, *92*, 7232.
(9) Ellermann, T.; Sehested, J.; Nielsen, O. J.; Wallington, T. J.; Pagsberg, P. *Chem. Phys. Lett.* **1993**, *218*, 287.
(10) Hippler, H. Private communication, 1993.
(11) Nielsen, O. J. Risø National Laboratory Report Risø-R-480, 1984.
(12) Ellermann, T. Risø National Laboratory Report Risø-M-2932, 1991.
(13) Wallington, T. J.; Ellermann, T.; Nielsen, O. J.; Sehested, J. *J. Phys. Chem.* **1993**, *98*, 2346.
(14) Sehested, J. *Int. J. Chem. Kinet.*, accepted for publication.
(15) Wallington, T. J.; Dagaut, P.; Kurylo, M. J. *Chem. Rev.* **1992**, *92*, 667.
(16) DeMore, W. B.; Sander, S. P.; Golden, D. M.; Molina, M. J.; Hampson, R. F., Jr.; Kurylo, M. J.; Howard, C. J.; Ravishankara, A. R.; Kolb, C. E. JPL Publication 92-20, 1992.
(17) Sehested, J.; Nielsen, O. J. Unpublished results.
(18) Uthman, A. P.; Sherman, G. A.; Takacs, G. A. *Spectrochim. Acta* **1977**, *34A*, 1109.
(19) Wallington, T. J.; Hurley, M. D.; Shi, J.; Maricq, M. M.; Sehested, J.; Nielsen, O. J.; Ellermann, T. *Int. J. Chem. Kinet.* **1993**, *25*, 651.
(20) Bedzhanyan, Y. R.; Markin, E. M.; Gershenzon, Y. M. *Kinet. Catal.* **1992**, *33*, 591.
(21) Nielsen, O. J.; Ellermann, T.; Sehested, J.; Bartkiewcz, E.; Wallington, T. J.; Hurley, M. D. *Int. J. Chem. Kinet.* **1992**, *24*, 1009.
(22) Brasseur, G.; Solomon, S. *Aeronomy of the Middle Atmosphere*; Reidel: Dordrecht, The Netherlands, 1986.
(23) Maricq, M. M.; Szente, J. J. *Chem. Phys. Lett.* **1993**, *213*, 449.